Nonlinear Cascades in Two-Dimensional Turbulent Magnetoconvection

Dan Škandera and Wolf-Christian Müller*

Max-Planck-Institut für Plasmaphysik, 85748 Garching, Germany

(Received 24 June 2008; published 3 June 2009)

The dynamics of spectral transport in two-dimensional turbulent convection of electrically conducting fluids is studied by means of direct numerical simulations in the frame of the magnetohydrodynamic Boussinesq approximation. The system performs quasioscillations between two different regimes of small-scale turbulence: one dominated by nonlinear magnetohydrodynamic interactions; the other governed by buoyancy forces. The self-excited change of turbulent states is reported here for the first time. The process is controlled by the ideal invariant cross helicity, $H^C = \int_S dS\mathbf{v}\cdot\mathbf{b}$. The observations are explained by the interplay of convective driving with the nonlinear spectral transfer of total magnetohydrodynamic energy and cross helicity.

DOI: 10.1103/PhysRevLett.102.224501 PACS numbers: 47.27.ek, 47.27.te, 52.30.−q

Turbulent convection of an electrically conducting fluid is of major importance for the dynamics of stellar convection zones and the evolution of magnetic fields in these regions. It is thus necessary to better understand its nonlinear dynamics which can be strongly influenced by advected temperature fluctuations and self-organization processes associated with the magnetic field. To this end the two-dimensional (2D) magnetohydrodynamic (MHD) Boussinesq approximation is applied as a simplified model that asymptotically describes the behavior of plasmas under the influence of a strong mean magnetic field directed perpendicular to the direction of gravity—a configuration, for example, realized in the filamentary sunspot penumbra [1] where the magnetic field is nearly horizontal and in laboratory plasma experiments. Additionally, convection represents a natural and more realistic way of sustaining turbulence when studying its inherent properties by numerical simulations in contrast to the somewhat artificial forcing mechanisms that are often applied in such studies. Buoyancy can turn the temperature field into an active scalar and, as a consequence, substantially modify the nonlinear spectral transport of energy and other ideal invariants by the respective turbulent cascade. Some progress has been made with regard to the understanding of homogeneous hydrodynamic turbulent convection, e.g., [2–10]. However, studies of convection in magnetofluids (see, e.g., [11] for a recent review) which focus on the small-scale properties of homogeneously turbulent states remain scarce.

This Letter deals with an investigation of the inertial-range dynamics of convectively driven two-dimensional MHD turbulence by direct numerical simulation. The system displays quasioscillatory changes between a state where turbulence is dominated by buoyant forces and a state governed by nonlinear MHD interactions. The constantly changing cross helicity, $H^C = \int_S dS\mathbf{v}\cdot\mathbf{b}$, is the cause for this behavior since it regulates the importance of MHD nonlinearities compared to buoyancy effects. The nonlinear interaction of the turbulent cascades of energy and cross helicity which leads to the self-excited alternation of turbulent regimes is reported here for the first time and yields further insight into the not yet fully understood dynamics of turbulent flows.

The system is described by the Boussinesq MHD equations (see, for example, [11]). In two dimensions with x denoting the horizontal and z the vertical direction they read

$$\frac{\partial\omega}{\partial t} + \mathbf{v}\cdot\nabla\omega - \mathbf{b}\cdot\nabla j = -\partial_x\theta + \nu\Delta\omega, \tag{1}$$

$$\frac{\partial\psi}{\partial t} + \mathbf{v}\cdot\nabla\psi = \eta\Delta\psi, \tag{2}$$

$$\frac{\partial\theta}{\partial t} + \mathbf{v}\cdot\nabla\theta = v_x + \kappa\Delta\theta, \tag{3}$$

$$\nabla\cdot\mathbf{v} = \nabla\cdot\mathbf{b} = 0, \tag{4}$$

where θ denotes temperature fluctuations about a mean gradient, $\mathbf{v}$ is the velocity of the flow, $\mathbf{b}$ is the magnetic field, $\omega = \mathbf{e}_y\cdot(\nabla\times\mathbf{v})$ stands for the vorticity, and ψ for the scalar magnetic potential, $\mathbf{b} = \nabla\psi\times\mathbf{e}_y$. The symbol $\mathbf{e}_y$ denotes the unit normal vector of the two-dimensional plane. The current density is given by $j = -\Delta\psi$. The dissipation coefficients ν, η, κ are dimensionless kinematic viscosity, resistivity, and thermal diffusivity, respectively. The equations are given in nondimensional form using a normalization to the time characteristic of large-scale buoyant motions $t_b = (\alpha g|\nabla T_0|)^{-1/2}$ and the temperature gradient scale $L_0 = T_*/|\nabla T_0|$. Here, α is the coefficient of thermal expansion, g is the gravitational acceleration acting in the negative z direction, and $T_0(x)$ is the mean linear temperature profile. The relevant definition for T_* is the root-mean-square (rms) value of temperature fluctuations (see, e.g., [12]). In contrast to the usual setup, ∇T_0 is in the horizontal direction in order to eliminate the elevator instability [10]. It otherwise appears due to periodic boundary conditions in the z direction and leads

to the formation of coherent vertical jets that significantly degrade the quality of turbulence statistics. A horizontal ∇T_0 leads to a large-scale x-dependent buoyancy force that cannot be balanced by the pressure gradient. Since this Letter concentrates on the small-scale dynamics of turbulence, the generation of large-scale vorticity by this effect is neglected in Eq. (1). The mean temperature gradient drives the turbulent flow [right-hand-side of Eq. (3), first term] by temperature fluctuations which couple with velocity fluctuations through the buoyancy force [right-hand-side of Eq. (1), first term]. The absence of magnetic dynamo action in 2D MHD [13,14] would necessitate explicit driving of magnetic field fluctuations. However, as the flow is homogeneously turbulent and thus does not concentrate the magnetic field on the boundaries of convection cells, the decay of magnetic energy is a slow process on the resistive time scale $t_D = L_0^2/\eta \gg t_b$. Thus, this quantity is quasistationary during the simulation which extends over 15 large-scale buoyancy times t_b.

The set of Eqs. (1)–(4) is solved on a 2π-biperiodic square using a standard pseudospectral method with dealiasing according to the 2/3 rule [15]. A simulation of the above-described setup is conducted with a resolution of 2048^2 collocation points. The initial state consists of randomly generated fields. The parameters of the run are set to $\nu = \eta = 7 \times 10^{-4}$ and $\kappa = 1.3 \times 10^{-4}$ which correspond to a Prandtl number $\mathrm{Pr} = \nu/\kappa \approx 5.4$ and a magnetic Prandtl number $\mathrm{Pr}_m = \nu/\kappa = 1$. The nominal Rayleigh number is $\mathrm{Ra} \approx 2 \times 10^6$. We note, however, that the value of the Ra characteristic of Rayleigh-Bénard systems with impermeable vertical boundaries is only of limited significance for the present periodic setup. All parameters are chosen such as to obtain comparable wave number intervals for the inertial ranges of the turbulent fields. The inherent anisotropy of the flow mainly affects the largest-scale fluctuations with wave numbers $k \leq 4$, while at smaller scales anisotropy becomes negligible. The total energy is given by $E = E^{\mathrm{MHD}} + E^{\theta}$ with $E^{\mathrm{MHD}} = E^K + E^M = 1/2 \int_S dS(v^2 + b^2)$ and the temperature "energy" $E^{\theta} = 1/2 \int_S dS\theta^2$. Analogously, the symbol $\varepsilon = \varepsilon_{\mathrm{MHD}} + \varepsilon_{\theta} = \int_S dS[(\mu\omega^2 + \eta j^2) + \kappa(\nabla\theta)^2]$ denotes the sum of dissipation rates of total magnetohydrodynamic energy and temperature energy. The turbulent state which develops quickly after the onset of convective instability is initially characterized by $E^K \approx 5.0$, $E^M \approx 6.0$, and $E^{\theta} \approx 1.9$. The values increase slowly by about 40% over the simulation period while staying in roughly constant ratios to each other.

In the observed energy spectra the signatures of two distinct turbulent regimes appear which quasiperiodically alternate. This happens in a continuous transition where either one or the other signature becomes more dominant. The time characteristic of the alternations and the duration of the clearest manifestation of the different states are of the order of t_b. The simulation period consists of two groups of time intervals labeled BO (Bolgiano-Obukhov) and IK (Iroshnikov-Kraichnan). Angle-integrated energy spectra, $E_k = \int d^3k' \delta(|\mathbf{k}'| - k) E(\mathbf{k}')$, obtained by time averaging over the group of IK intervals are shown in Fig. 1. The spectrum of total MHD energy denoted by the solid line exhibits IK behavior, $E_k^{\mathrm{MHD}} \sim k^{-3/2}$ [16,17], in the inertial range of scales, $5 \lesssim k \lesssim 20$. The spectrum is normalized by $(\varepsilon_{\mathrm{MHD}} b_0)^{1/2}$ with b_0 being the rms magnetic field, and it displays a constant prefactor $C_{\mathrm{IK}} \approx 1.8$ that agrees well with previous work on 2D MHD turbulence (see, e.g., [18]). The spectra of E^K and E^M (not shown) exhibit comparable amplitudes and scaling consistent with the IK picture. Although the validity of this 2D MHD turbulence phenomenology is still a matter of controversy due to its neglect of anisotropy caused by the magnetic field, direct numerical simulation of two-dimensional MHD turbulence [18,19] appears to agree well with it.

The temperature energy spectrum E_k^{θ} displays a somewhat shorter scaling range, $5 \lesssim k \lesssim 12$, with an exponent of $-5/3$. The Obukhov-Corrsin scaling suggests that temperature fluctuations are passively advected by the velocity field. Note that this does not necessarily imply the same scaling for kinetic energy, which in fact scales closer to $k^{-3/2}$. The spectrum of the mean square magnetic potential (not shown) scales self-similarly over the same spectral interval as E_k^{MHD} with $|\psi_k|^2 \sim k^{-7/2}$, consistent with magnetic field fluctuations under the influence of large-scale driving, $|\psi_k|^2 \sim E_k^{\mathrm{MHD}} k^{-2}$ [20]. Thus, during the IK phases the effects of buoyancy on the flow are negligible compared to the MHD nonlinearities which clearly dominate nonlinear dynamics.

Angle-integrated energy spectra obtained by time averaging over the BO intervals are depicted in Fig. 2.

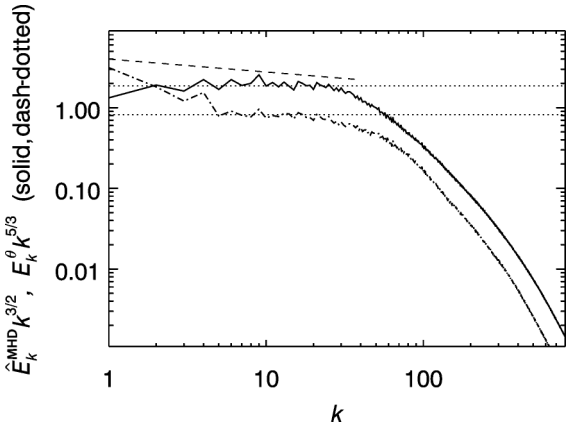

FIG. 1. Angle-integrated spectra of normalized MHD energy, $\hat{E}_k^{\mathrm{MHD}} = E_k^{\mathrm{MHD}}/(b_0 \varepsilon_{\mathrm{MHD}})^{1/2}$, compensated by $k^{3/2}$ (solid line), and temperature "energy," E_k^{θ}, compensated by $k^{5/3}$ (dash-dotted line), time averaged over the IK intervals. The dashed line indicates $k^{-5/3}$ scaling with regard to $\hat{E}_k^{\mathrm{MHD}}$; the dotted horizontal lines mark scaling law prefactors.

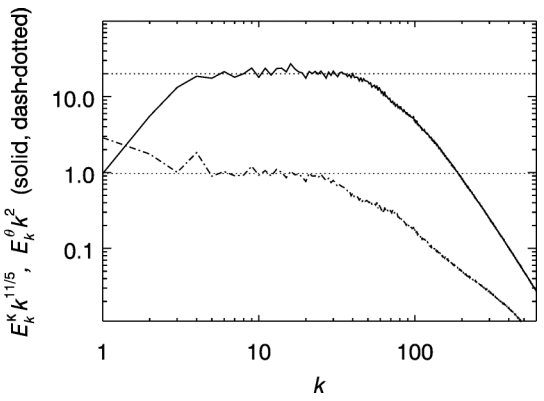

FIG. 2. Angle-integrated spectra of kinetic energy, E_k^K, compensated by $k^{11/5}$ (solid line), and temperature energy, E_k^θ, compensated by k^2 (dash-dotted line). Both spectra are time averaged over the BO intervals of the simulation. Same meaning for dotted lines as in Fig. 1.

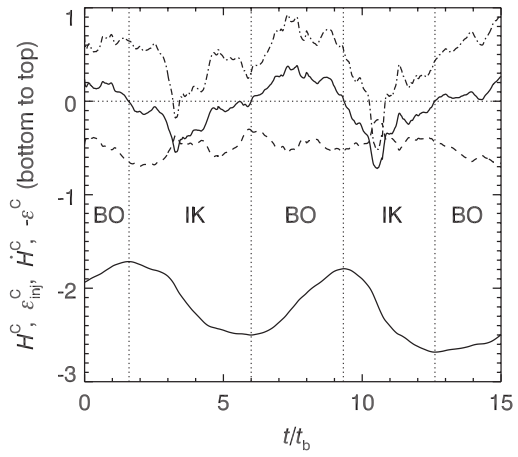

FIG. 3. Time evolution of H^C (lower solid line), $\dot{H}^C$ (upper solid line), the associated flux injected by convective driving $\varepsilon_{\rm inj}^C$ (dashed line), and the negative dissipation rate $-\varepsilon^C$ (dash-dotted line). The intervals of IK and BO states are indicated.

Although E_k^K (solid line) is not an ideal invariant of MHD the spectrum scales with the exponent $-11/5$ for $4 \lesssim k \lesssim 40$, while for the temperature energy (dash-dotted line) approximately $E_k^\theta \sim k^{-2}$ is obtained. No clear scaling behavior is exhibited by $E_k^{\rm MHD}$ and E_k^M. In the BO picture of convective turbulence [21,22] the temperature field can drive velocity fluctuations. As opposed to hydrodynamic turbulence, spectral transfer is not characterized by the turnover time at scale l, $t_{\rm NL} \sim l/v_l$, but by the scale-dependent buoyancy time, $t_b^* \sim (l/\theta_l)^{1/2}$. Consequently, $E_k^\theta \sim k^{-7/5}$ and $E_k^K \sim k^{-11/5}$. The observed scaling of E_k^K is in good agreement with the respective BO law, in contrast to the behavior of E_k^θ. Hydrodynamic test runs with similar parameters exhibit BO behavior for both fields. The spectra shown in Fig. 2 suggest that the investigated system operates in a modified buoyancy-dominated Bolgiano-Obukhov-like regime. The buoyancy force dominates nonlinear MHD interactions in the inertial range; i.e., the temperature is an active scalar significantly influencing the energy transfer.

The time intervals of both turbulent regimes are correlated with the evolution of total cross helicity H^C as depicted in Fig. 3. It is important to note that other physical quantities, e.g., the energies or the turbulent heat flux, fluctuate on different time scales and are not correlated with the quasioscillations. A simulation run with lower resolution 1024^2 confirms the stability of the phenomenon for at least $100t_b$. The dissipation coefficients of this test run are set to $\nu = 1.5 \times 10^{-3}$, $\eta = 7.5 \times 10^{-4}$, $\kappa = 4 \times 10^{-4}$. The impact of cross helicity in a strongly aligned turbulent system like in this simulation with $\rho = \langle|\mathbf{v}\cdot\mathbf{b}|\rangle/(4E^K E^M)^{1/2} \in [0.8, 0.95]$ on the nonlinear dynamics of MHD turbulence is known to lead to significant modifications of spectral energy transfer [23,24]. The limiting case $\rho = 1$ corresponds to an Alfvénic state where the nonlinear dynamics is completely switched off. The effect of weakening of nonlinear MHD interactions in high cross-helicity states of turbulence is the key ingredient in following considerations.

In contrast to plain MHD turbulence, cross helicity in magnetoconvective turbulence is not an ideal invariant, as can be seen from $\dot{H}^C = \int_S \theta b_z dS - (\nu + \eta)\int_S j\omega dS = \varepsilon_{\rm inj}^C - \varepsilon^C$. The dissipative term ε^C has a larger effect at small scales due to the appearance of spatial derivatives, whereas the term $\varepsilon_{\rm inj}^C$ injects cross helicity predominantly at large scales. The interplay between all three terms of the cross-helicity balance in the performed simulation is shown in Fig. 3. The time intervals of IK turbulence can be identified with negative $\dot{H}^C$ (upper solid line), whereas the time intervals of BO-like turbulence are correlated with positive $\dot{H}^C$. The term $\varepsilon_{\rm inj}^C$ (dashed line) is always negative, permanently injecting negative cross helicity into the system. Figure 3 shows that if the negative small-scale cross-helicity dissipation $-\varepsilon^C$ (dash-dotted line) becomes larger than the absolute amount of the injected cross helicity, $|\varepsilon_{\rm inj}^C|$, the system switches from the IK state to the BO state and vice versa.

In the following, an explanation for the quasioscillations is proposed. It is assumed that at the beginning the system operates in the IK regime. This choice is not essential, but provides a convenient starting point for the ensuing considerations. The IK regime implies that inertial-range energies and energy fluxes associated with Elsässer variables $\mathbf{z}^\pm = \mathbf{v} \pm \mathbf{b}$ are approximately equal [25]; i.e., $E^+ \approx E^-$ with $E^\pm = 1/4\int_S dS(z^\pm)^2$ and for the corresponding direct nonlinear spectral fluxes $T_k^+ \approx T_k^-$. Consequently, total cross helicity, $H^C = E^+ - E^-$, and the associated nonlinear flux in the inertial range, $T_k^{H^C} = T_k^+ - T_k^- \approx \varepsilon^+ - \varepsilon^-$, are minimal. Nonlinear MHD interactions are dominant in the inertial range (see Fig. 4). However, the

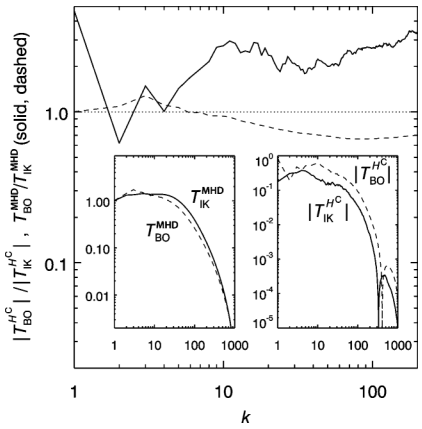

FIG. 4. Ratio of nonlinear spectral energy fluxes of MHD energy $T_k^{\mathrm{MHD}} = \int_k^{k_{\max}} dk' \{\mathbf{v} \cdot [-\mathbf{v} \cdot \nabla \mathbf{v} + \mathbf{b} \cdot \nabla \mathbf{b} - \nabla P] + \mathbf{b} \cdot [\nabla \times (\mathbf{v} \times \mathbf{b})]\}_{k'}$ (dashed line) and cross helicity $T_k^{H^C} = T_k^+ - T_k^- = 1/2 \int_k^{k_{\max}} dk' \{-\mathbf{z}^+ \cdot [\mathbf{z}^- \cdot \nabla \mathbf{z}^+ + \nabla P] + \mathbf{z}^- \cdot [\mathbf{z}^+ \cdot \nabla \mathbf{z}^- + \nabla P]\}_{k'}$ (solid line) time averaged over IK and BO intervals with the total pressure $P = p + b^2/2$ and $\{\bullet\}_k$ denoting Fourier transformation. Insets display the spectral fluxes with $T_k^{H^C} > 0$ for $k \lesssim 300$ and negative beyond.

convective driving continuously generates negative cross helicity at the rate $\varepsilon_{\mathrm{inj}}^C$, predominantly at largest scales. The apparently delayed adaption of the initially depleted direct nonlinear transfer of cross helicity leads to an accumulation of H^C at large scales. The resulting growth of the $|H^C|$ breaks the balance of E^+ and E^- and, consequently, weakens nonlinear MHD interactions together with the resulting spectral flux of E^{MHD} as shown in Fig. 4. Thus, the process gives rise to inertial-range dynamics dominated by buoyancy forces. Therefore, simultaneously with the growth of H^C the dynamics of the system changes toward the buoyancy dominated BO-like regime of turbulence.

In the BO-like regime, due to $E^+ \neq E^-$, the corresponding spectral fluxes T_k^+ and T_k^- are different. Hence, the spectral flux $T_k^{H^C}$ and cross-helicity dissipation ε^C are larger. Thus, the BO-like regime leads to efficient annihilation of the accumulated cross helicity. As H^C decreases, the system approaches Elsässer energy equipartition, $E^+ \approx E^-$, and it returns to the IK regime of 2D magneto-convective turbulence. Because of the continuous injection of cross helicity by large-scale convection, the magnetic and velocity field of the flow are highly aligned. The same phenomenon could not be observed in topologically less constrained three-dimensional simulations.

In summary, self-excited quasioscillations between an Iroshnikov-Kraichnan regime and a Bolgiano-Obukhov-like regime of turbulence are observed in two-dimensional direct numerical simulation of homogeneous MHD Boussinesq turbulence. The highly aligned turbulent fields, a consequence of the convective large-scale driving, give rise to a quasiperiodic weakening of nonlinear MHD interactions in favor of buoyancy effects. The resulting Bolgiano-Obukhov-like regime allows the removal of cross helicity by nonlinear spectral transfer strengthening the MHD nonlinearities again. The two distinct turbulent states emerge due to the nonlinear interplay of the cascades of energy and cross helicity, a situation of general importance to MHD systems constrained by the presence of a strong mean magnetic field as found, e.g., on the Sun.

The authors thank M. Proctor for an important remark regarding the simulation setup.

*Wolf.Mueller@ipp.mpg.de

[1] J. H. Thomas and N. O. Weiss, Annu. Rev. Astron. Astrophys. **42**, 517 (2004).
[2] I. Procaccia and R. Zeitak, Phys. Rev. Lett. **62**, 2128 (1989).
[3] A. Brandenburg, Phys. Rev. Lett. **69**, 605 (1992).
[4] S. Toh and E. Suzuki, Phys. Rev. Lett. **73**, 1501 (1994).
[5] E. Suzuki and S. Toh, Phys. Rev. E **51**, 5628 (1995).
[6] D. Biskamp and E. Schwarz, Europhys. Lett. **40**, 637 (1997).
[7] V. S. L'vov, Phys. Rev. Lett. **67**, 687 (1991).
[8] S. Grossmann and V. S. L'vov, Phys. Rev. E **47**, 4161 (1993).
[9] A. Celani, T. Matsumoto, A. Mazzino, and M. Vergassola, Phys. Rev. Lett. **88**, 054503 (2002).
[10] E. Calzavarini, D. Lohse, F. Toschi, and R. Tripiccione, Phys. Fluids **17**, 055 107 (2005).
[11] M. R. E. Proctor, in *Fluid Dynamics and Dynamos in Astrophysics and Geophysics*, edited by A. M. Soward, C. A. Jones, D. W. Hughes, and N. O. Weiss (CRC Press, Boca Raton, FL, 2005), p. 235.
[12] M. Gibert, H. Pabiou, F. Chillà, and B. Castaing, Phys. Rev. Lett. **96**, 084501 (2006).
[13] Y. B. Zeldovich, Sov. Phys. JETP **4**, 460 (1957).
[14] T. G. Cowling, Vistas Astron. **1**, 313 (1955).
[15] C. Canuto, M. Y. Hussaini, A. Quarteroni, and T. A. Zang, *Spectral Methods in Fluid Dynamics* (Springer-Verlag, New York, 1988).
[16] P. S. Iroshnikov, Astron. Zh. **40**, 742 (1963) [Sov. Astron. **7**, 566 (1964)].
[17] R. H. Kraichnan, Phys. Fluids **8**, 1385 (1965).
[18] D. Biskamp and E. Schwarz, Phys. Plasmas **8**, 3282 (2001).
[19] D. Biskamp and H. Welter, Phys. Fluids B **1**, 1964 (1989).
[20] A. Pouquet, J. Fluid Mech. **88**, 1 (1978).
[21] R. Bolgiano, J. Geophys. Res. **67**, 3015 (1959).
[22] A. M. Obukhov, Dokl. Akad. Nauk SSSR **125**, 1246 (1959).
[23] R. Grappin, U. Frisch, J. Léorat, and A. Pouquet, Astron. Astrophys. **105**, 6 (1982).
[24] R. Grappin, A. Pouquet, and J. Léorat, Astron. Astrophys. **126**, 51 (1983).
[25] M. Dobrowolny, A. Mangeney, and P. Veltri, Phys. Rev. Lett. **45**, 144 (1980).